



Effects of Layer Characteristics on the Properties Of Three-Layer Particleboards

Robert L. Geimer

H. M. Montrey

William F. Lehmann

Abstract

Three-layer particleboards were constructed in three thicknesses, using both random and oriented face flake alignment. Face layer density and consequently board bending stiffness increased with an increase in either face weight or board thickness. Face density was further altered by "steam shock" methods. The resulting fast closure increased face density at the expense of flake bonding quality. Graphs are included showing the dependency of board effective MOE on the amounts and types of core and face material. Linear expansion is compared for boards having aligned and random face flakes. Bending stiffness predictions made with mathematical formulas developed for three-layer and multilayer particleboards were verified by several test methods. Results show that variation in stiffness predictions using layer characteristics is comparable to variation experienced within board properties and test methods.

FROM BOTH ECONOMICAL AND ENGINEERING CONSIDERATIONS, a desirable particleboard configuration for many structural applications is a three-layer construction wherein poorer material is utilized in the core, and strong, stiff flakes comprise the faces. The relation which layer characteristics and associated process variables have in regard to effective panel stiffness has been studied in varying detail by a number of researchers (see bibliography).

The purposes of this study were to: a) Observe the effects of certain variables on layer characteristics, b) determine to what degree the face-core characteristics of density, thickness, and stiffness influence the physical properties and dimensional stability of a structural composite board, and c) develop and verify methods of predicting stiffness based on layer properties.

Experimental Design

Three-layer boards, 24 by 28 inches, were constructed using 3/4-inch pulp chips (cut to 0.020-in.

flakes in a ringflaker) as the core material, and 0.020- by 0.5- by 2-inch flakes produced by a disk flaker for the face. Boards were made in three thicknesses (1/2, 3/4, and 1 inch), each with two face weights (0.167 and 0.333 lb./ft.²) on each face (ovendry (OD) weight basis). Ratios of face weight to total weight thus were dependent on board thickness, and varied in the three-layer configurations from a low of 10 percent in the 1-inch boards to a high of 40 percent in the 1/2-inch boards (Table 1). Homogeneous boards using all core material were made to serve as controls.

Board construction factors were as follows:

Species	: Douglas-fir
Panel density ¹	: 40 lb./ft. ³ (OD weight, volume at test)
Face and core resin	: 5 percent liquid phenolic (based on OD weight of flakes)
Wax	: 1 percent (based on OD weight of flakes)
Moisture content (mat)	: 10 percent
Press temperature	: 350°F
Presstime	: 10 minutes for 1/2-inch boards; 12 minutes for 3/4-inch boards; and 15 minutes for 1-inch boards
Closure time	: 1 minute

Part of the variation in physical properties of particleboards can be attributed to variations in the density gradients occurring throughout the board thickness.

In order to examine these variations, a second set of boards, with relatively high and low density faces,

¹This represents the panel weight per unit volume—not a density, per se, because of the composite nature of layered board constructions.

The authors are Technologist, Engineer, and Technologist, respectively, USDA Forest Service, Forest Products Lab., Madison, Wis. This paper was presented at Session 29 - Particleboard & Molded Products - of the 28th Annual Meeting of the Forest Products Research Society, June 27, 1974, in Chicago, Ill. It was received for publication in October 1974.

Table 1. — PHYSICAL PROPERTIES OF THREE-LAYER, DOUGLAS-FIR PARTICLEBOARDS.

Board thickness and description ¹	Closure time	Double face-total weight ratio ²	OD SG ³	Thickness	IB	MOE	MOE ⁴	Face layers				Core				
								OD SG ³	Thickness		Tension		OD SG	Tension MOE	Interlaminar	
									Single ⁵	Double or percent of total thickness	Strength	MOE			Shear strength	MOE
(min.)	(%)	(in.)	(lb./in. ²)	(lb./in. ²)	(lb./in. ²)	(1,000 lb./in. ²)	(in.)	(lb./in. ²)	(1,000 lb./in. ²)	(1,000 lb./in. ²)	(1,000 lb./in. ²)	(1,000 lb./in. ²)	(1,000 lb./in. ²)			
40 lb./ft.³																
1/2 in. .000 (all core)	1	—	0.592	0.536	107	2,450	395	—	—	—	—	—	—	—		
.167 random	1	20	.613	.539	94	3,060	521	0.690	0.046	17.2	967	455	0.592	371	305	29.9
.333 random	1	40	.636	.532	103	4,090	607	.742	.086	32.4	1,886	721	.573	390	304	29.8
.333 random ⁶	0.25	40	.630	.512	152	3,860	692	.783	.083	32.0	1,971	695	.540	358	398	36.8
.333 random	2	40	.636	.524	140	3,770	586	.665	.096	36.8	1,596	531	.615	480	450	40.7
3/4 in.																
.000 (all core)	1	—	.655	.790	93	3,310	500	—	—	—	—	—	—	—	—	—
.167 random	1	13.3	.623	.783	117	3,380	615	.730	.044	11.2	1,526	676	.601	395	326	28.9
.333 random	1	26.6	.631	.776	147	4,110	893	.803	.080	20.6	3,036	923	.570	408	353	34.4
.333 random ⁶	0.33	26.6	.621	.771	142	3,600	484	.822	.078	20.7	2,331	828	.565	380	352	34.9
.333 random	2	26.6	.629	.774	163	3,750	612	.670	.095	24.6	1,942	583	.611	462	411	37.6
1 in.																
.000 (all core)	1	—	.640	—	66	3,150	526	—	—	—	—	—	—	—	—	—
.167 random	1	10	.646	1.020	103	3,820	629	.826	.039	7.2	2,122	721	.623	398	271	32.6
.333 random	1	20	.647	1.026	101	4,170	666	.859	.075	14.4	2,867	855	.611	404	281	28.9
.333 random ⁶	0.5	20	.607	1.028	84	3,270	630	.858	.075	14.4	2,101	773	.557	356	222	23.0
.333 random	4	20	.647	1.028	113	3,470	607	.677	.095	18.4	1,515	591	.639	463	285	28.7
1/2 in.																
.167 aligned parallel	1	20	.628	.532	113	3,860	895	.696	.046	17.2	2,551	1,301	.609	416	357	35.2
perpendicular	1	20	.628	.532	113	3,500	347	.696	.046	17.2	324	134	.609	416	357	35.2
.333 aligned parallel	1	40	.652	.522	110	6,740	1,394	.770	.083	32.0	3,640	1,809	.573	388	327	30.3
perpendicular	1	40	.652	.522	110	3,050	340	.770	.083	32.0	392	181	.573	388	327	30.3
3/4 in.																
.167 aligned parallel	1	13.3	.616	.785	128	4,240	963	.755	.042	10.8	3,448	1,657	.598	392	324	34.7
perpendicular	1	13.3	.616	.785	128	2,930	444	.755	.042	10.8	566	224	.598	392	324	34.7
.333 aligned parallel	1	26.6	.639	.785	144	5,990	1,283	.776	.082	21.4	4,771	2,102	.566	404	369	36.7
perpendicular	1	26.6	.639	.785	144	2,500	334	.776	.082	21.4	587	186	.566	404	369	36.7
1 in.																
.167 aligned parallel	1	10	.637	1.021	101	3,870	866	.825	.039	7.6	4,342	1,809	.615	371	283	29.9
perpendicular	1	10	.637	1.021	101	3,500	503	.825	.039	7.6	678	233	.615	371	283	29.9
.333 aligned parallel	1	20	.636	1.021	104	4,920	1,097	.847	.076	14.8	4,943	2,147	.585	384	273	28.5
perpendicular	1	20	.636	1.021	104	2,790	426	.847	.076	14.8	722	244	.585	384	273	28.5
30 lb./ft.³																
3/4 in. 0.167 aligned parallel	1	17.8	.441	.782	62	1,870	501	.525	.061	15.6	2,110	1,151	.425	210	150	15.4
perpendicular	1	17.8	.441	.782	62	1,290	220	.525	.061	15.6	221	72	.425	210	150	15.4
.333 aligned parallel	1	35.6	.504	.766	74	4,150	936	.631	.101	26.4	2,345	1,296	.450	233	166	15.3
perpendicular	1	35.6	.504	.766	74	1,020	150	.631	.101	26.4	330	84	.450	233	166	15.3

¹Decimal indicates single-face spread in lb./ft.³; random and aligned refer to face flake orientation.
²Face material—0.020- by 0.5- by 2-inch disk-cut flakes; core material—3/4-inch pulp chips cut to 0.020 inch thick in ring-type flaker.
³Based on OD weight and volume at 80°F and 65 percent relative humidity.
⁴Single-point loading on 24:1 span for 1/2- and 3/4-inch-thick boards; 18:1 on 1-inch boards.
⁵Computed from specific gravity measurements and known face weights.
⁶Boards made with fast closure had "steam shock" treatment.

was constructed by using either a fast or slow closure rate. Mat moisture distribution was regulated in the fast closure boards to further increase the face density. This consisted of reducing the core moisture to 5 percent, keeping the face moisture at 10 percent, and adding an additional 3 percent moisture in the form of

water spray on the top and bottom faces. Closure times varied with each thickness (Table 1). Except for closure time and mat moisture content (MC), board construction factors were as described above.

Another series of boards having aligned face flakes was constructed in the three thickness

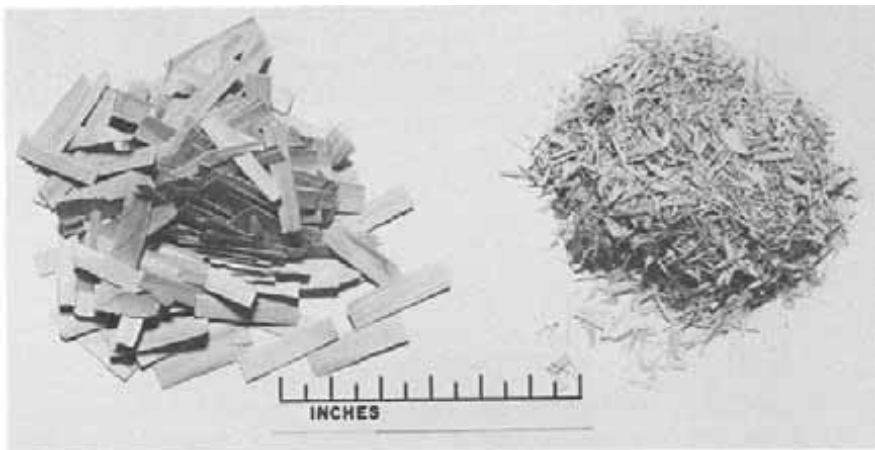


Figure 1. — Flake types used to construct experimental three-layer structural particleboards. At the left, face flakes, 0.02-inch by 0.5-inch by 2-inch, are from a disk flaker. At the right, core material is 3/4-inch pulp chips flaked to 0.02-inch thick, in a ring flaker.

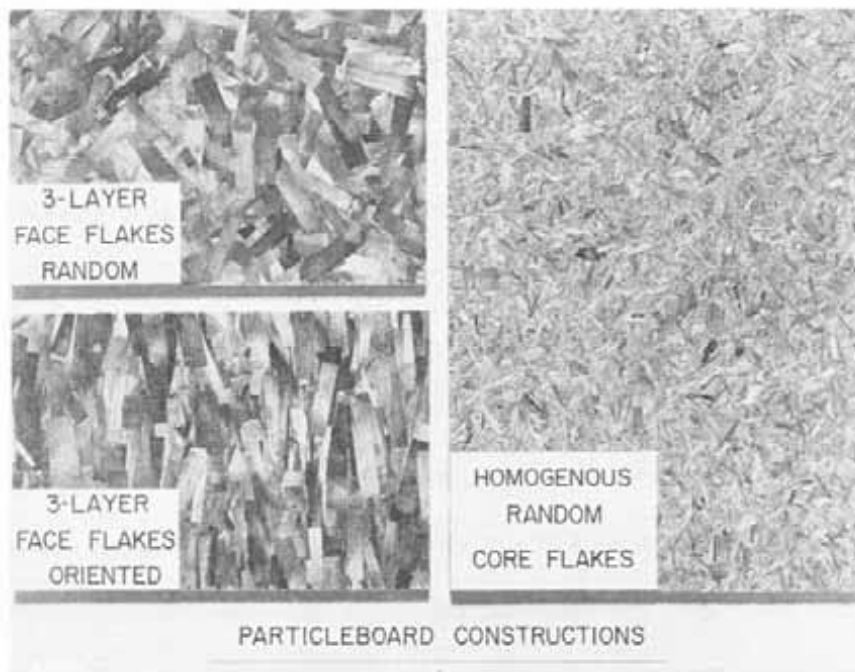


Figure 2. – Surface appearance of the three board types used in study.

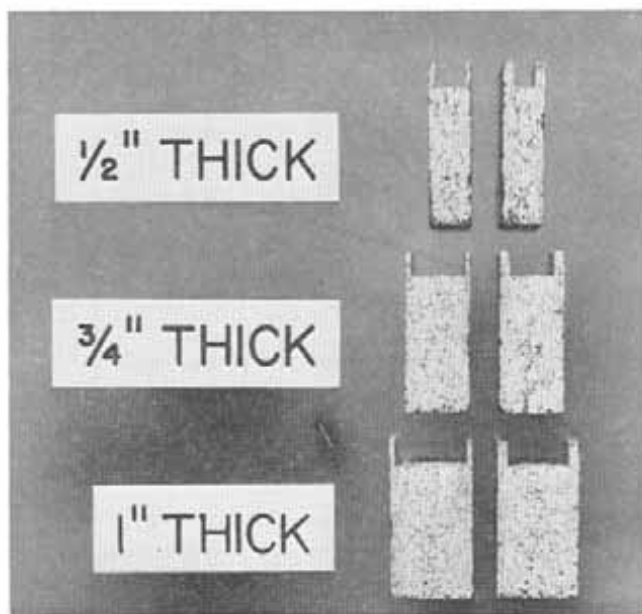


Figure 3. – Face-core relationships for boards of each thickness.

categories with face weights of 0.167 and 0.333 lb./ft.². Closure time was 1 minute.

Finally, a set of 3/4-inch-thick boards having aligned face flakes was constructed at a density of 30 lb./ft.³ with face weights of both 0.167 and 0.333 lb./ft.². Here again other board construction factors remained as described previously. Figures 1, 2, and 3

illustrate raw material, board types, and thickness variations.

Four boards were made of each aligned construction (the exception was that only one board was made for each face weight in the 30 lb./ft.³ series) and duplicate boards were made of random construction. Duplication of test samples within a board resulted in test averages based on a minimum of four specimens.

Testing

Boards were tested for specific gravity (SG), modulus of rupture (MOR), bending stiffness yielding effective modulus of elasticity (MOE), and internal bond (IB) according to ASTM D 1037 (1). (Exceptions were that bending specimens from 1-inch-thick panels were tested on an 18-inch span instead of a 24-inch span, and all deflections were measured with a yoke-transducer apparatus supported on the bending specimen instead of being measured with apparatus supported on the testing machine.) Additional bending tests were made using two-point loading on an 18-inch span. These data were used to develop and verify methods of predicting stiffness from layer characteristics.

Face and core layers were separated in one series of specimens and tested for stiffness in tension parallel to the board surface. Core layers were also tested in interlaminar shear to determine their flatwise shear modulus values.

All boards were retested for SG, MOR, MOE, and IB following a standard ASTM D 1037 (1) accelerated-aging test. The dimensional stability properties of linear expansion, thickness swell, and water absorption were determined between oven-dry (OD) and vacuum-pressure-soak (VPS) conditions.

Table 2. — RESPONSE OF THREE-LAYER DOUGLAS-FIR PARTICLEBOARDS TO ENVIRONMENTAL CONDITIONING.

Board thickness and description ¹	Closure time (min.)	Double face-total weight ratio ² (%)	Accelerated aging (percent of original values)				Spring-back (%)	Dimensional stability OD-VPS (percent increase from original)		
			OD	IB	MOR	MOE		Linear expansion	Thick-ness swelling	Water soak
			SG							
40 lb./ft.³										
1/2 in., 0.000 (all core)	1	—	76	41	66	64	22	0.37	32	124
.167 random	1	20	75	43	69	75	23	.38	29	122
.333 random	1	40	77	36	75	81	23	.37	25	115
.333 random	0.25	40	80	42	77	77	18	.38	19	105
.333 random	2	40	79	35	83	88	20	.32	25	107
3/4 in., .000 (all core)	1	—	76	20	65	70	22	.48	30	108
.167 random	1	13.3	80	16	76	78	20	.33	27	104
.333 random	1	26.6	80	13	80	85	19	.40	25	102
.333 random	0.33	26.6	79	23	75	77	18	.34	20	104
.333 random	3	26.6	80	25	82	91	18	.35	20	103
1 in., .000 (all core)	1	—	74	4	27	53	24	.48	28	110
.167 random	1	10	78	7	62	71	19	.42	22	101
.333 random	1	20	81	16	69	74	17	.40	23	105
.333 random	0.5	20	81	11	64	66	21	.37	22	103
.333 random	4	20	77	6	66	70	18	.38	23	104
1/2 in., .167 aligned parallel	1	20	73	37	64	65	23	.18	31	117
perpendicular	1	20	73	37	60	59	23	.45	31	117
.333 aligned parallel	1	40	74	41	67	69	21	.15	28	110
perpendicular	1	40	74	41	43	57	21	.70	28	110
3/4 in., .167 aligned parallel	1	13.3	81	16	70	72	19	.22	25	106
perpendicular	1	13.3	81	16	75	78	19	.44	25	106
.333 aligned parallel	1	26.6	80	21	67	74	20	.15	24	104
perpendicular	1	26.6	80	21	67	71	20	.66	24	104
1 in., .167 aligned parallel	1	10	80	9	71	68	18	.24	21	104
perpendicular	1	10	80	9	61	65	18	.43	21	104
.333 aligned parallel	1	20	78	10	59	60	19	.15	22	102
perpendicular	1	20	78	10	60	60	19	.48	22	102
30 lb./ft.³										
3/4 in., 0.167 aligned parallel	1	17.8	—	22	—	—	—	—	—	—
perpendicular	1	17.8	—	22	—	—	—	—	—	—
.333 aligned parallel	1	35.6	—	27	—	—	—	—	—	—
perpendicular	1	35.6	—	27	—	—	—	—	—	—

¹Decimal indicates single-face spread in lb./ft.²; random and aligned refer to face flake orientation.

²Face material—0.020- by 0.5- by 2-inch, disk-cut flakes; core material—3/4-inch pulp chips cut to 0.020 inch thick in ring-type flaker.

Results

Face Layer Specific Gravity

Tables 1 and 2 summarize measured data. Required precision in determining face layer thickness could not be attained by simple measurements, as visual determination of exact face and core boundaries was complicated by minor spreading variations and intermixing of face and core material. The best measure of face layer thickness was found to be that computed from specific gravity measurements and face layer weights.

Face layer specific gravity data are presented graphically in Figure 4. Average face layer specific gravity is dependent on total board thickness, face weight, and, of course, total board density. Figure 5 presents the same data in a perspective for comparison of the 3/4-inch boards of different densities. The

relative effect of board thickness and face layer weight is nearly the same regardless of board density.

The effect of closure rate (as mentioned previously) on the board density gradient is shown for 3/4-inch boards in Figure 6. The density gradient existing in any hot-pressed particleboard is related to the relative flatwise crushing strength of various layers of the mat. The crushing strength of the layers progressively decreases with exposure to increasing temperature or MC or both, as occur during the initial stages of hot pressing. Because temperature transfer is time-dependent, fast rates of closure necessarily accent density gradients while slow closure rates tend to even out or reduce severe density differences.

Average face layer specific gravity is also affected by the amount of face material. Depending on the general shape of the density gradient curve as deter-

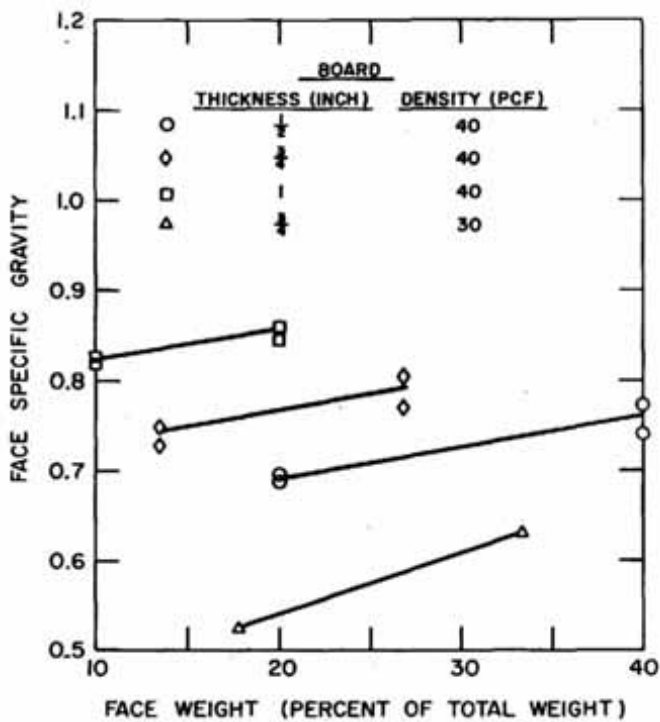


Figure 4. - Face layer specific gravity as affected by amount of face weight and total thickness.

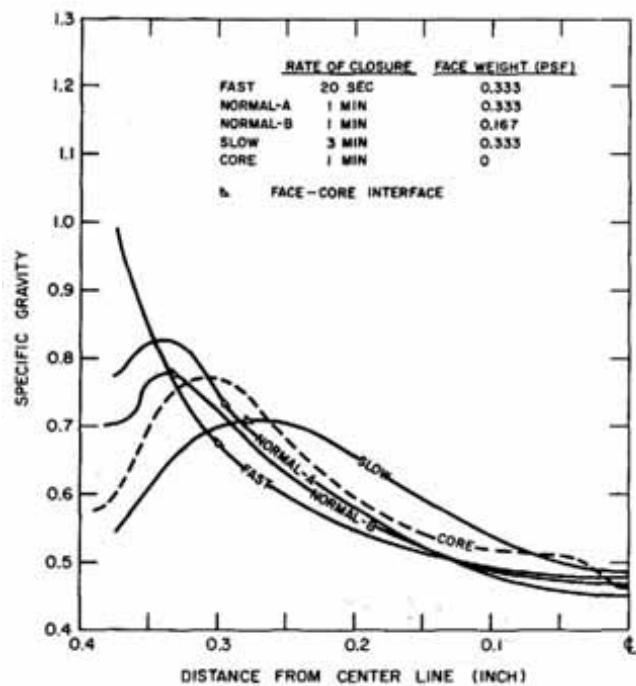


Figure 6. - Density gradient for 3/4-inch particleboards as affected by rate of closure and face weight.

mined by press closure, the average face-layer density may be increased or decreased with an increased use of face material. On a rising density gradient representative of a board made with a slow closure, an increase in amount of face material causes a shift of the face-core interface to a higher spot on the curve, and, consequently, average face specific gravity increases.

Increasing face material in a board made with a fast closure (falling density gradient curve) moves the face-core interface farther down the curve and lowers average face specific gravity.

Face density is also affected by the type of face material used. In this experiment, the large face flakes retard moisture (and therefore heat) transfer. Increasing the percentages of face material, then, serves to raise the density gradient curve and consequently increase average face layer density. This is illustrated in Figure 6 for boards made with 0.167 lb./ft.² (normal B) and 0.333 lb./ft.² (normal A) face material.

Thicker boards will necessarily have steeper density gradients (and therefore higher average face layer specific gravities) due to the longer time required for surface temperatures and moisture to penetrate the board.

Specific Gravity/Stiffness

Face layer tensile stiffness (MOE, tension) varies in a nonlinear manner with specific gravity. The relationship is shown in Figure 7. A rather substantial increase in tensile stiffness accompanies increases in specific gravity above 0.75. Flake alignment served to increase tensile stiffness in the direction of alignment to 2.5 to 3.5 times that of random configurations.

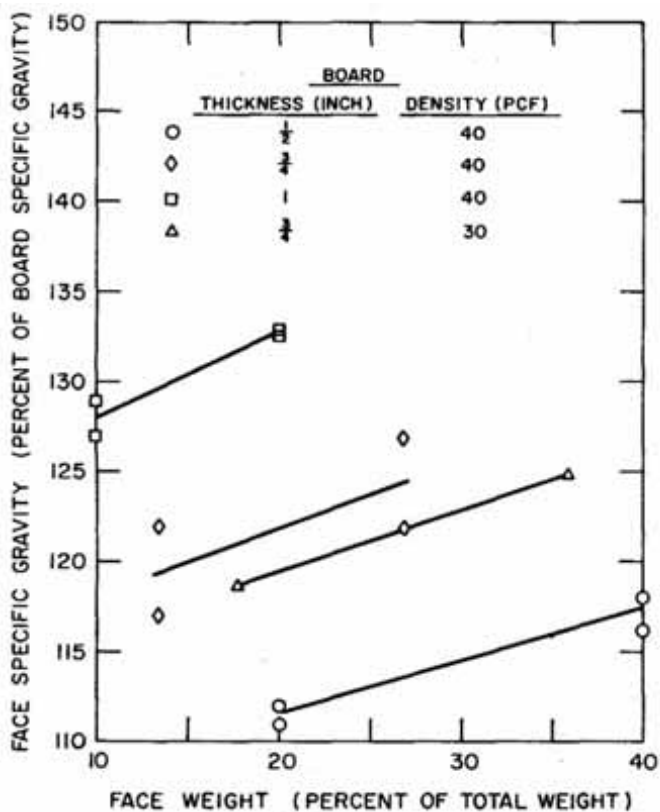


Figure 5. - Face specific gravity/board specific gravity plotted against face weight/board weight ratio.

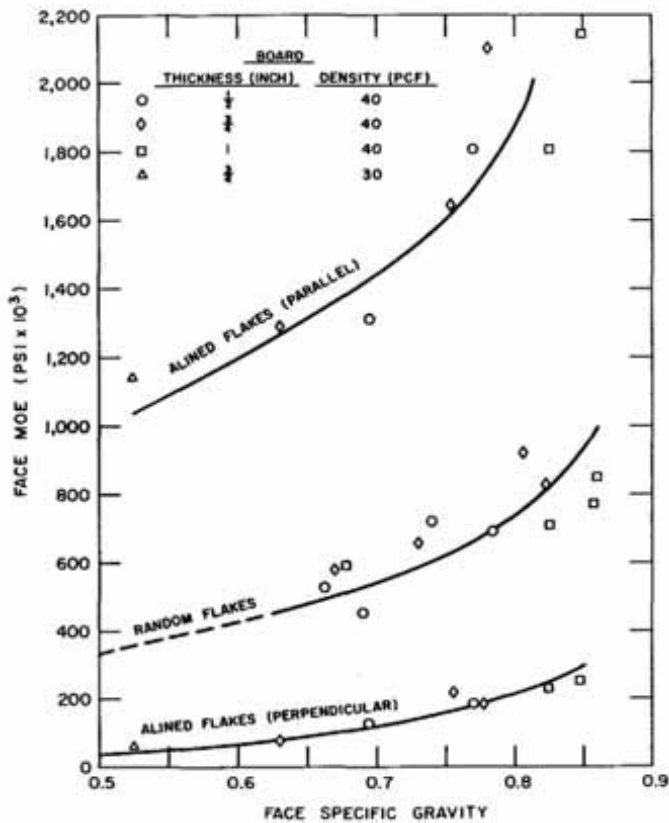


Figure 7. - Influence of SG on the MOE (tensile) properties of particleboard face layers.

When moisture was added to the faces and the press was closed rapidly, face specific gravity was increased, but face stiffness decreased. This can be attributed to weak glue bonds between face flakes caused by starved joints. Also, since the face is denser than normal, any surface overcure which occurs will affect a greater proportion of the total face material.

Increasing face density necessarily lowers core density for a given board density. However, the average change is not extreme if the core is more than 50 percent of the board thickness. The relationship between core specific gravity and core MOE (tension) is shown in Figure 8.

Predicting Board Stiffness

The deflection of a three-layer board can be predicted using the theory describing structural sandwich constructions. In particular

$$\Delta = k_s \frac{Pa^3}{bD} + k_r \frac{Pa}{bU} \quad [1]$$

where

- Δ = deflection.
- D = bending stiffness per unit board width.
- U = shear stiffness per unit board width.
- P = total load applied to the specimen,
- a = span of the specimen,
- b = specimen width.

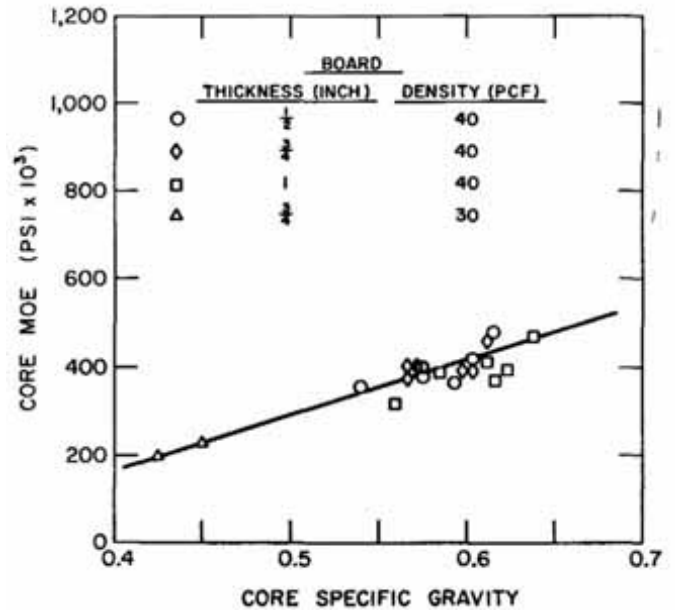


Figure 8. - Influence of SG on the MOE (tensile) properties of particleboard cores.

k_b, k_s = coefficients, whose values are determined by the type of flexural loading.

The first term in the deflection expression represents bending deflections, while the second term represents shear deflections.

In a discrete three-layer board, D can be calculated from the properties and dimensions of the individual layers. In particular,

$$D = \frac{1}{E_1 t_1 + E_2 t_2 + E_c t_c} \left[E_1 t_1 E_2 t_2 h^2 + \frac{E_1 t_1 E_c t_c (t_1 + t_c)^2}{4} + \frac{E_2 t_2 E_c t_c (t_2 + t_c)^2}{4} \right] + \frac{1}{12} [E_1 t_1^3 + E_2 t_2^3 + E_c t_c^3] \quad [2]$$

where, following the notation of Figure 9,

- E_1, E_2 = MOE of faces 1 and 2, respectively.
- t_1, t_2 = thickness of faces 1 and 2, respectively.
- E_c = MOE of the core.
- t_c = thickness of the core.
- $h = t_c + 1/2(t_1 + t_2)$ = distance separating the facing midplanes.

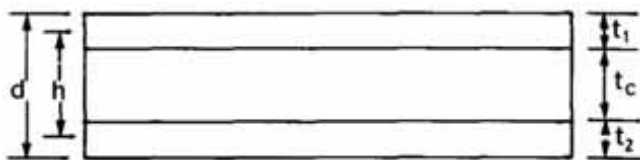
If the top and bottom faces have identical values of MOE, E , and thickness, t , Equation [2] becomes:

$$D = \frac{E}{12} (d^3 - t^3) + \frac{E_c t^3}{12} \quad [3]$$

where d = total board thickness.

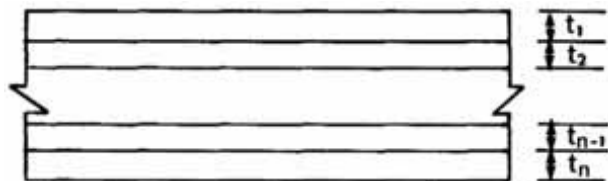
Bending stiffness D can also be expressed in terms of a moment of inertia and an "effective" MOE representing the board. That is,

$$D = \frac{E_e d^3}{12} \quad [4]$$



3 Layer

- d, Total thickness
- h, Distance between facing midplanes
- t_1, t_2 , Face layer thickness
- t_c , Core thickness



Multilayer

- t_1, t_2, \dots, t_n , first, second, and n^{th} layer thickness

Figure 9. – Three-layer and multilayer constructions.

where E' is the “effective” MOE of the board—not a true material “property,” but an indicator of bending stiffness.

Shear stiffness U is related to the core properties and becomes significant in predicting flexural deflections of a three-layer board only if the bending stiffness of the faces is appreciably greater than the shear stiffness of the core, or if the span between the supports is relatively short.

Shear stiffness can be approximated by

$$U = hG_c \quad [5]$$

where

G_c = core “flatwise” MOR, associated with shear deformations in planes perpendicular to the board face.

Face layer tension MOE was determined on specimens from both faces, in both principal directions, of each board type. The data were used to compute a “predicted” D using Equation [2] wherein individual layer characteristics were handled separately, and again with Equation [3] wherein thickness and MOE values for the individual faces were combined and averaged. In all cases the predicted values of D obtained by each method agreed within 1 percent. “Predicted” values of D presented in Table 3 are those obtained by averaging top and bottom face thickness and MOE.

Flatwise MOR was determined on core specimens for each board and the “predicted” shear stiffness, U , was calculated using Equation [5]. Values of U are shown in Table 3. Using corresponding values of D and U it can be shown using the expressions of Equation [1] that shear deflections are quite small compared to bending deflections for beams having span-depth ratios at or above 18:1 (a spandepth ratio of 24:1 is commonly used in testing board products). Shear stiffness U was, therefore, unimportant in predicting deflections for the boards investigated.

Measuring Stiffness

To determine the validity of the “predicted” values for bending, flexure tests were performed on specimens cut from each principal direction of each board. The load-deflection ratios were measured and the data used to determine a “measured” bending stiffness, D . Since shear stiffness was negligible in controlling deflections during flexure, that portion of Equation [1] containing the U factor can be eliminated, and “measured” D becomes:

$$D = k_B \frac{a^3}{b^3} \left(\frac{P}{\Delta} \right) \quad [6]$$

Two types of flexure tests were performed on each specimen:

1) Two-point loading on an 18-inch span with load points at specimen third-points. Constants for this loading arrangement are $k_B=23/1296$ and $k_s=1/6$.

2) The standard ASTM D 1037 (1) method (with the exception noted below) for testing particleboard with single-point loading on a 24:1 spandepth ratio (because of specimen size limitations, the 1-inch boards were tested on an 18-inch span). Constants are $k_B=1/48$ and $k_s=1/4$. Because of the long span, this method minimizes the effect of shear stiffness and the data serve as a check against the first method.

The ASTM loading arrangement was used to determine maximum bending strength. A yoke-transducer apparatus supported on the specimen, as described in ASTM standard test specification C 393 (2), was used to monitor loaddeflection behavior in both modes of testing.

Included in Table 3 are data showing the precision of predicted stiffness measurements. Predicted values averaged 78 percent, and ranged from 63 to 110 percent of the two-point loading method data. The predicted values were closer to the ASTM single-point loading method data (average 87; range 72 to 120 percent); however, variation in the precision of predicting results of either test method was essentially the same (coefficient of variation 13 and 12 percent, respectively), indicating that both testing methods had the same relative repeatability. Measured bending stiffness values obtained from the ASTM single-point loading tests were, of course, lower than those obtained by the two-point loading tests, due to the marked effect of concentrated loads on midspan deflections during single-point loading of relatively “soft” materials such as particleboard.

Predicted stiffness values were closer to measured values for certain board types—notably those with a

Table 3. — PREDICTED AND MEASURED VALUES OF STIFFNESS, D.

Board thickness and description		Closure time	Three-layer analysis				Multilayer analysis			
			Predicted U from core properties	Average predicted D from layer properties	Ratio predicted D to measured D		Single sample predicted D from layer properties	Ratio predicted D to measured D		
					Two-point loading, 18-inch span	Center loading		Two-point loading, 18-inch span	Center loading	
(min.)	(lb./in.)	(lb.-in. ³ /in.)	(%)	(%)	(%)	(%)				
1/2 in.,	0.167 random	1	15,040	5,220	70	79	6,300	87	95	
	.333 random	1	13,210	7,650	88	101	7,940	92	106	
	.333 random	0.25	15,850	6,590	75	85	9,030	107	122	
	.333 random	2	17,340	6,140	78	88	4,890	72	70	
3/4 in.,	.167 random	1	21,310	18,860	68	76	22,790	81	90	
	.333 random	1	23,840	25,730	88	96	28,620	104	112	
	.333 random	0.33	24,010	22,560	80	87	29,920	104	119	
	.333 random	3	25,380	20,230	76	86	18,920	73	83	
1 in.,	.167 random	1	31,670	41,030	63	74	57,890	92	108	
	.333 random	1	29,880	51,870	77	87	65,470	99	110	
	.333 random	0.50	20,950	46,180	73	81	70,100	107	125	
	.333 random	4	26,710	46,870	77	86	49,410	82	90	
Average of boards with random face flakes					75	85		92	102	
Coefficient of variation					9	9		14	17	
1/2 in.,	0.167 aligned	parallel	1	17,180	9,900	74	87	—	—	—
		perpendicular	1	17,120	3,800	78	85	—	—	—
	.333 aligned	parallel	1	13,290	15,710	80	95	—	—	—
		perpendicular	1	13,180	2,960	93	104	—	—	—
3/4 in.,	.167 aligned	parallel	1	25,520	28,190	64	74	—	—	—
		perpendicular	1	25,600	15,060	74	84	—	—	—
	.333 aligned	parallel	1	25,400	49,500	95	99	—	—	—
		perpendicular	1	25,780	12,190	83	91	—	—	—
1 in.,	.167 aligned	parallel	1	29,340	57,100	65	74	—	—	—
		perpendicular	1	29,330	32,250	67	72	—	—	—
	.333 aligned	parallel	1	26,850	89,730	82	93	—	—	—
		perpendicular	1	26,800	31,700	78	84	—	—	—
3/4 in.,	.167 aligned	parallel	1	10,950	23,890	110	120	—	—	—
	perpendicular	1	11,140	6,390	67	72	—	—	—	
30 lb./ft. ³	.333 aligned	parallel	1	10,280	32,700	80	91	—	—	—
		perpendicular	1	10,080	4,950	85	88	—	—	—
Average of all boards					78	87	—	—	—	
Coefficient of variation					13	12	—	—	—	

face weight of 0.333 lb./ft.² and 1 minute press closure. This is related to how closely actual density gradients correspond to average values as shown previously in Figure 6 for 3/4-inch boards.

Multilayer Analysis

As is noted above, the density gradient within each board was not that of a truly discrete three-layer construction (i.e., a sandwich construction). With the goal of more exactly predicting bending stiffness characteristics, the utility of a multilayer analysis model was investigated.

A laminated construction having an arbitrary number of layers, *n*, is pictured in Figure 9. Prediction of the bending stiffness, *D*, of such a construction involves two steps: Location of the section neutral axis and calculation of the sum of the bending stiffnesses

of all individual layers about the neutral axis. Of course, if the construction is symmetric, the neutral axis is located at the geometric center of its cross section.

Thickness and MOE of the *i*th layer are denoted by *t_i* and *E_i*, respectively. The distance, *y*, defining the location of the neutral axis relative to the top surface of the layered construction can be written (3) as

$$\bar{y} = \frac{\sum_{i=1}^n E_i t_i c_i}{\sum_{i=1}^n E_i t_i} \quad [7]$$

where *c_i* locates the neutral axis of layer *i* relative to the top surface.

After determination of the neutral axis location using Equation [7], the bending stiffness, D , can be calculated from

$$D = \sum_{i=1}^n E_i I_i \quad [8]$$

where I_i is the moment of inertia per unit width of layer i relative to the neutral axis located by Equation [7].

The specific gravity gradient was determined when successive 1/32-inch layers were removed from boards having randomly oriented face flakes. The specific gravity values of the face layers were used in conjunction with the empirical SG-MOE data of Figure 7 to obtain MOE values for these lamina. Similarly, MOE values for lamina cut from core material were obtained by combining SG measurements for these lamina with the data of Figure 8.

An n -layered model was thus "assembled" for these boards, each layer having a thickness and corresponding MOE. Equations [7] and [8] were then utilized to predict the bending stiffness, D , for each of these multilayered constructions. In addition, the thickness and MOE values for lamina located symmetrically relative to the board section's geometric center were averaged and a resultant symmetric multilayered model was assembled. The bending stiffness, D , for these symmetrically layered models was predicted, using Equation [8], with $\bar{y}=d/2$. As was the case for predicted values obtained using the three-layer model, negligible difference occurred between the D values obtained from the symmetric and unsymmetric constructions. Table 3 compares predicted D values with those "measured" using both types of loading. Predictions made using a multilayer analysis did prove to be closer, on an average, to measured values than those made with the three-layer method (102 percent vs. 85 percent, respectively, for the ASTM single-point loading method and 92 percent vs. 75 percent for the two-point loading method). However, the variation in precision of prediction was increased slightly. Statistical interpretation is necessarily limited as the multilayer analysis was based on measurements taken from a single board in each case.

A comparison of multilayer and three-layer analysis for board types differing in density gradients is shown in Table 4. Differences in prediction results were greatest in those board types having a rapid density change in the outermost layer.

MOE Variations in Board Types

The extent to which density gradients are controlled by material bulk density was not explored in this work. However, unpublished data accumulated at the Forest Products Laboratory over several years show how the effective board stiffness (MOE) is affected by the amount and type of material in three-layer boards. These data are presented graphically in Figures 10, 11, and 12. Figure 10 shows the MOE properties of a planer shavings board as modified with increasing amounts of different types of face material.

Thirty percent face material accounts for 60 to 85 percent of the stiffness increase possible if the boards were constructed of all face material.

Figure 11 is a plot of data obtained during the current study showing MOE as affected by board thickness. Here, a 1/2-inch board utilizing 30 percent face material gains 40 percent of the possible stiffness increase, while using the same proportion of material in a 1-inch board achieved 48 percent of the possible gain. This difference can be accounted for by the higher face specific gravity in the 1-inch board, as

Table 4. — STIFFNESS PREDICTION PRECISION FOR CERTAIN BOARD TYPES COMPARING THREE-LAYER AND MULTILAYER ANALYSIS METHODS.

Board type	Closure time	Average of ratios, predicted D to measured D (two-point method)		Difference (%)
		Three-layer	Multilayer	
0.167 lb./ft. ³ face weight	1 min.	67	87	+20
.333 lb./ft. ³ face weight	1 min.	84	98	+14
.333 lb./ft. ³ face weight	Fast	76	106	+30
.333 lb./ft. ³ face weight	Slow	77	76	-1

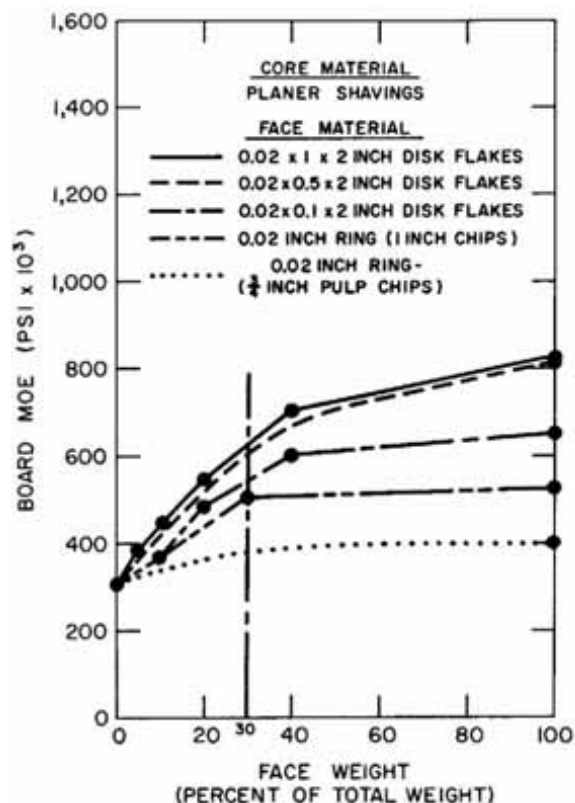


Figure 10. - MOE of three-layer boards showing the effect of face flake quality and quantity on planer shavings core.

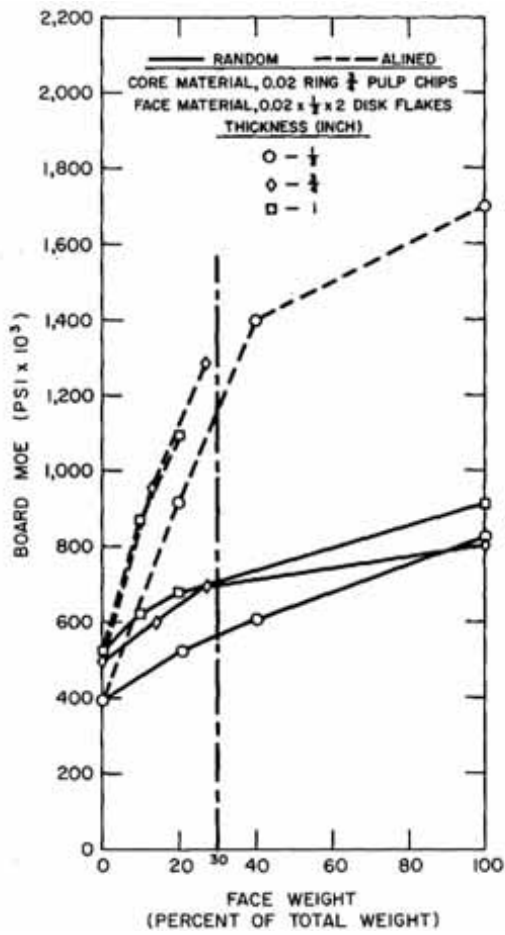


Figure 11. - MOE of three-layer boards showing the effect of board thickness and face flake alignment.

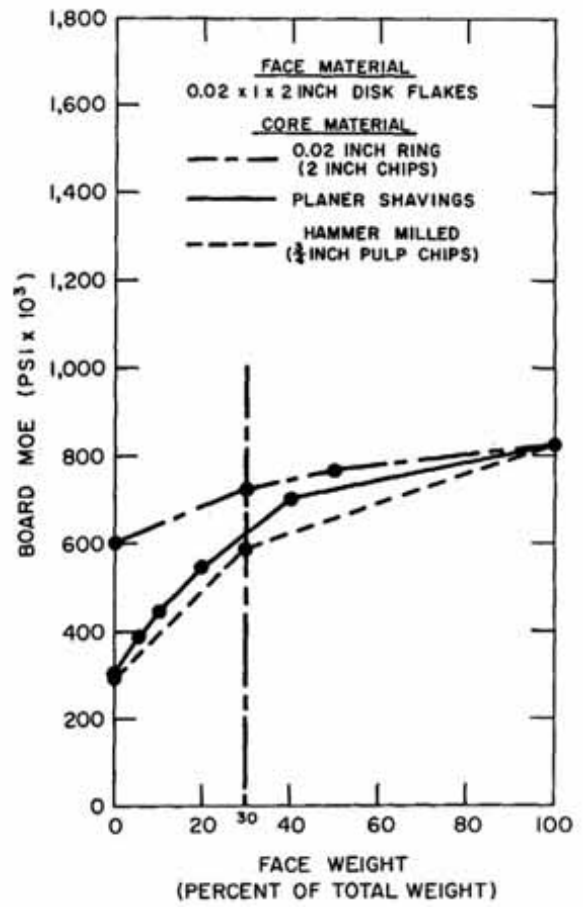


Figure 12. - MOE of three-layer boards showing the effect of using different cores with a high-quality face flake.

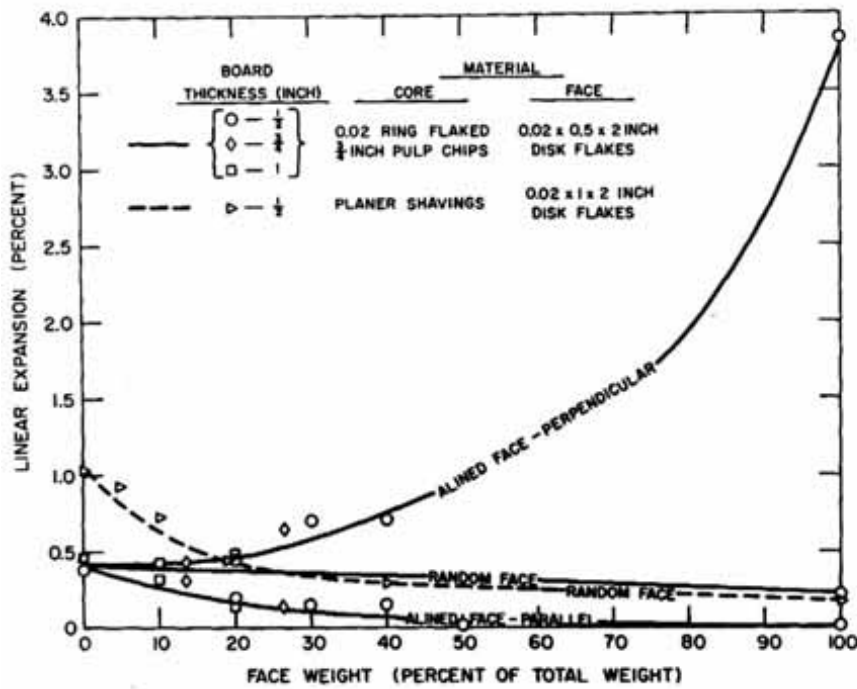


Figure 13. - OD-VPS linear expansion of three-layer particleboards.

previously discussed. The effect with aligned face flakes was more pronounced. One-half-inch boards with 30 percent face material reached 60 percent of the possible stiffness gain.

Figure 12 shows MOE of boards utilizing the same face but having different core materials. Here, use of 30 percent face material achieved between 52 and 60 percent of the total possible stiffness gain.

Durability and Dimensional Stability

Surprisingly, within the range of the 40 lb./ft.³ boards, no correlation existed between initial average core SG and IB, either before or after accelerated aging.

Linear expansion (OD-VPS) for the random board type under study was decreased only slightly by the addition of face flakes, since the difference in linear expansion of an all-face board and an all-core board was slight (face-0.2percent; core-0.37to 0.48 percent). Linear expansion is quite extreme, of course, across the grain of an aligned board and varies with the amount of face material, as shown in Figure 13. A 40 percent face layer addition may be used before the perpendicular-to-the-grain linear expansion exceeds CS 236-66 (4) limits for class 2-B-2.² For comparative purposes a linear expansion curve is shown for a board with a planer shavings core and random face flakes.

In general, the three-layer boards had slightly less thickness swelling than the all-core boards. Thickness swelling and water absorption values averaged 24 and 106 percent, respectively. Except for a slight increase of these values in the thinner aligned boards, no statistically important differences occurred among three-layer board types.

Conclusions

Within the parameters of the materials used and three-layer board types constructed in this study, it has been found that:

1) SG of the face layers increases with an increase in the amount of face material and with board thickness. The relation is attributed to retardation of moisture movement and heat transfer and the position of the face-core interface relative to the high-density portion of the density gradient curve.

2) Face layer density-board density ratios remain nearly constant, regardless of total board densities, if face weight-total weight ratios and board thickness remain the same.

3) Face layer stiffness increases in a nonlinear fashion with face SG for both aligned and nonaligned flakes.

4) Fast-closing combined with "steamed shock" treatments, though increasing face SG, may be detrimental to stiffness properties of the face layer and consequently the total board.

5) Stiffness of the composite board may be predicted from its layer thicknesses and stiffness

²OD-VPS linear expansion is approximately 3 times the expansion measured from 50 to 90 percent relative humidity.

characteristics. Prediction precision varies with the type of board and the refinements of analysis.

6) A 30 percent addition of high-quality face flakes will result in achieving more than 30 percent of the possible gain in MOE. The amount of increase is in part dependent on the type of materials used and on board thickness.

7) A 40 percent addition of aligned face flakes to a nonaligned core can be made before linear expansion perpendicular to the grain becomes excessive.

Literature Cited

1. AMERICAN SOCIETY FOR TESTING AND MATERIALS. 1972. Tests for evaluating building fiberboards. ASTM Desig. D 1037-72A. ASTM, Philadelphia, Pa.
2. ———. 1962. Flexure test of flat sandwich constructions. ASTM Desig. C 393-62. ASTM, Philadelphia, Pa.
3. U. S. DEPARTMENT OF AGRICULTURE. 1955. Wood Handbook. USDA Agri. Handb. 72. USDA Forest Service, Forest Products Lab., Madison, Wis. pp. 282-284.
4. U. S. DEPARTMENT OF COMMERCE. 1966. Mat-formed wood particleboard. U.S. Com. Stand. CS 236-66. National Bureau of Standards, Office of Product Standards, Washington, D.C.

Bibliography

- DENISOU, O. 1973. The control of the pressing process in the production of particleboard. *Holztechnologie* 14(1):43-46.
- DESCULTU, H., and I. DUMITRU. 1967. The optimum ratio between the moisture content of glued chips in the surface layers and in the core of particleboard. *Industr. Lemn.* 18(5):161-165.
- FUJII, J. S. 1958. The effect of overlay materials on the flexure properties of commercial particleboard. *Forest Prod. J.* 18(8):219-222.
- GAMOU, V. 1973. Static bending strength of wood particleboard. *IZU UUZ Lesnoi ZH* 16(1):115-118.
- HEFTY, F. 1967. Exploring effects of press closing rates on strength properties and specific gravity gradients of particleboards. Unpublished report. USDA Forest Service, Forest Prod. Lab., Madison, Wis.
- HUNT, M. 1970. Predictions of the elastic constants of particleboard by means of a structural analogy. Thesis, North Carolina State Univ., Raleigh, N.C.
- JAYNE, B. 1972. Theory and design of wood and fiber composite materials. Syracuse Univ. Press, Syracuse, N.Y. 418 pp.
- KEYLWERTH, R. 1958. On the mechanics of multilayer particleboard. *Holz als Roh- und Werkstoff* 16(11):419-430.
- KLAR, G. V., and J. STOFKO. 1965. High strength, composite wood particleboards. *Drevo* 20(1):5-7,18.
- KUSIAN, R. 1968. Model studies on the influence of chip size on the structural and strength properties of chip products (2) experimental studies. *Holztechnol.* 9(4):241-248.
- MAY, H. A. 1970. Effects of control of the pressing process on the economics and quality of particleboard manufacture. *Holz als Roh- und Werkstoff* 28(10):391-396.
- OTLEU, I. A. 1971. Changes in the moisture content of particleboard mats during hot pressing. *Derevoobrabat Prom.* 20(10):3-4.
- PLATH, E. 1971. Particleboard mechanics. *Holz als Roh- und Werkstoff* 29(10):377-382.
- . 1972. The computation of wood base sandwich boards. *Holz als Roh- und Werkstoff* 30(2):57-61.
- SCHEDRO, D. A. 1972. Wood particleboard pressing pressure. *Derevoobrabat Prom.* (9):7-8.
- SOSNIN, M., and M. KLIMOUA. 1971. Determining the elastic resistance of the chip mat during pressing. *Forestry Abs.*, Vol. 34; abstract No. 2553. 1973.
- STOFKO, J. 1962. Flakeboard material with directed wood chips. *Drevarsky Uyskum* (2):127-146.
- STRICKLER, M. 1959. Effect of press cycles and moisture content on properties of Douglas-fir flakeboard. *Forest Prod. J.* 9(7):203-215.
- SUCHSLAND, O. 1960. An analysis of a two-species three-layer wood flakeboard. *Quart. Bull., Mich. Agri. Expt. Sta., East Lansing, Mich.* 43(2):375-393.
- . 1962. The density distribution in flakeboards. *Quart. Bull. Mich. Agri. Expt. Sta., East Lansing, Mich.* 45(1):104-121.
- ZUBAN, P. 1969. Effect of mat density and particle dimensions on the gas permeability of a chip mat. *Forestry Abs.*, Vol. 33; abstract No. 3503. 1972.
- . 1969. Effect of nonuniform density on the gas permeability of a chip mat. *Forestry Abs.*, Vol. 33; abstract No. 3504. 1972.